

Enabling Quick, Accurate Crowdsourced Annotation for Elevation-Aware Flood Extent Mapping

Landon Dyken¹, Saugat Adhikari², Pravin Poudel³, Steve Petruzza³, Da Yan², Will Usher⁴, Sidharth Kumar¹

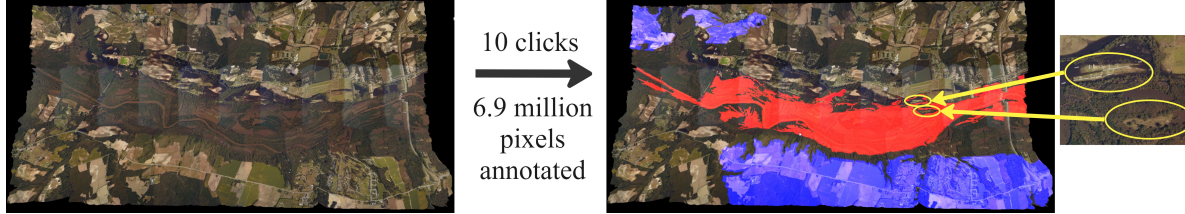


Fig. 1: An annotation made on a 6500×3000 pixel aerial image of flooding caused by Hurricane Matthew using only ten clicks of our topological segmentation tool. Pixels overlaid with blue have been labeled as dry and red as flooded. Note that areas labeled as flooded can appear green on the left, this is due to the tree canopy obscuring the flooded ground beneath. This tool guides annotation using the corresponding elevation data for a region, resulting in accurate labels. This can be seen by the highlighted areas where the tool annotated flooding around small dry features, but left them unlabeled. In our experimental user study, we show that this tool is more efficient than the state-of-the-art elevation-guided tool and can be used effectively by untrained participants.

Abstract—In order to assess damage and properly allocate relief efforts, mapping the extent of flood events is a necessary and important aspect of disaster management. In recent years, deep learning methods have evolved as an effective tool to quickly label high-resolution imagery and provide necessary flood extent mappings. These methods, though, require large amounts of annotated training data to create models that are accurate and robust to new flooded imagery. In this work, we provide FloodTrace, an application that enables effective crowdsourcing for flooded region annotation for machine learning training data, removing the requirement for annotation to be done solely by researchers. We accomplish this through two orthogonal methods within our application, informed by requirements from domain experts. First, we utilize *elevation-guided* annotation tools and 3D rendering to inform user annotation decisions with digital elevation model (DEM) data, improving users' annotation accuracy. For this purpose, we provide a unique annotation method that uses topological data analysis to outperform the state-of-the-art elevation-guided annotation tool in efficiency. Second, we provide a framework for researchers to review aggregated crowdsourced annotations and correct inaccuracies using methods inspired by uncertainty visualization. We conducted a user study to confirm our application's effectiveness in which 266 graduate students annotated high-resolution aerial imagery from Hurricane Matthew in North Carolina. Experimental results show the accuracy and efficiency benefits of our application apply even for untrained users. In addition, using our aggregation and correction framework, flood detection models trained on crowdsourced annotations were able to achieve performance equal to models trained on expert-labeled annotations, while requiring a fraction of the time on the part of the researcher. Our solution is completely web-based for ease of access with a demo available at <https://ldyken53.github.io/threejs-floodmap/>.

1 INTRODUCTION

In recent years, the societal impact of flooding has been difficult to ignore, with the severity and frequency of flood events increasing year after year [20]. In response, mapping the extent of these floods has become a crucial tool in a multitude of domains, from disaster response and insurance risk assessment to urban planning and agriculture.

As flood extent mapping continues to grow in importance, the amount of data being gathered on flooded regions has also grown, with it now being unfeasible to expect manual labeling of flood extent to meet necessary demand. To address this, it has become common for much smaller amounts of labeled data to be used to train classification models which can then quickly perform this task on new data as it is collected. Many classification models based on deep learning techniques have shown effectiveness for flood extent mapping by utilizing satellite imagery, unmanned aerial vehicle (UAV) data, hydrographs, and digital elevation model (DEM) data [4].

Although these models greatly reduce the area of flooded regions that need to be manually labeled, they still require annotated training sets to effectively learn from. High accuracy within training sets is paramount to allow dependent models to correctly learn and predict flooding. Producing these annotations requires a huge time commitment

for domain scientists, which becomes prohibitive for creating the large, varied datasets necessary to train models that can reliably respond to unseen flooded imagery. While fully expert-labeled training data is the standard, crowdsourcing offers a powerful way to gather annotated datasets, and has been shown before as a valuable tool for emergency response [21, 26] and mapping floods specifically [11, 42, 60].

Existing flood annotation datasets are most commonly created by manual labeling of aerial imagery with simple brushes and polygon selection tools, which is extremely time-consuming. Semi-automatic approaches improve a user's productivity by allowing them to label larger areas more quickly with the assistance of a guiding algorithm. Semi-automatic tools have been used previously to create flood annotation datasets [8, 24, 42, 51] through various algorithms on the flooded imagery being labeled. While these tools can improve productivity, our work builds on insight from domain experts which motivates a focus on *elevation-guided* annotation of flooded regions. The state-of-the-art machine learning models in this domain are physics-guided and take into account the elevation of the region being observed by utilizing Digital Elevation Model (DEM) data [34, 37, 46, 53, 68]. These models require very accurate ground truth labels for training. This is especially true for areas of high and low relative elevation in a dataset, and for adjacent pixels with very different elevation, named border pixels. With these models, a high-elevation pixel that is mislabeled as flooded can cause many surrounding pixels to be incorrectly inferred as flooded. By supplementing aerial imagery data with corresponding DEM data, the annotation process can be guided by elevation and lead to more accurate

¹University of Illinois Chicago, ²Indiana University Bloomington, ³Utah State University, ⁴Luminary Cloud

rate training data for dependent models. Moreover, elevation data can inform the labeling of otherwise ambiguous pixels covered by clouds and tree canopies.

In this work, we propose FloodTrace, a system for quick, accurate annotation that improves researchers’ workflows and enables high-quality crowdsourcing for flood extent mapping. Our design was informed by insight from domain experts in the form of repeated meetings and demos with one senior and two junior researchers working on machine learning models for flood extent mapping. Because flooding is naturally related to the varying elevation of land in an area, we take advantage of DEM data to inform annotation decisions with 3D views and tools, building a fully *elevation-guided* annotation application. We provide state-of-the-art and novel semi-automatic annotation tools that utilize elevation data and topological data analysis to increase annotation speed and accuracy. In our evaluation, we show that these tools can be used effectively by untrained students as proof of crowdsourcing potential.

FloodTrace is designed to encourage and improve the quality of crowdsourcing for this domain. Because of this, our solution is implemented as an interactive web application, making it easily accessible for end users. To improve researcher trust and understanding, our application provides an uncertainty visualization component to visualize aggregated crowdsourced annotations and find areas of high uncertainty between annotators. Annotation tools can then be used to directly correct those regions, improving the quality of aggregated annotations as training data.

To evaluate FloodTrace, we conducted a user study with 266 computer science graduate students in which we logged all interactions and results over several annotation tasks. Aggregated annotations were then used to train elevation-aware machine learning models, which were tested for flood detection on unseen regions to assess training data quality. We find that elevation-guided tools increased the accuracy of participants’ annotations, while our topological segmentation tool greatly increased annotation efficiency. We show that by using our aggregate visualization and correction workflow, crowdsourced annotations can be used to create models with equal performance to models trained on expert-labeled annotations, while requiring a fraction of the effort on the part of the researcher. Our contributions are:

- A novel framework for accurately annotating flooded regions using both satellite imagery and elevation data. Effective tools in a web-based application enable easy and productive crowdsourcing.
- A visualization component for reviewing and correcting crowdsourced annotations by showing uncertainty between annotators.
- An evaluation of our framework’s performance through a user study with 266 participants.
- The dataset of annotations from the user study, consisting of 1,321 unique annotations on eight distinct regions of North Carolina during Hurricane Matthew. Average dimensions of each annotation were 2573×1284 pixels. Annotations are provided with their metadata at [anonymized link].

2 BACKGROUND AND RELATED WORK

In this section, we first discuss the workflow of machine learning researchers to provide context for how our application can improve existing methods for flood extent mapping (Sect. 2.1). Then, we investigate previous work in crowdsourcing applications to motivate and inform our design (Sect. 2.2) and review related work in annotation tools (Sect. 2.3). Finally, we motivate and give background for the topological data analysis methods used for our novel elevation-guided annotation tool (Sect. 2.4).

2.1 ML for Flood Extent Mapping Workflow

While workflows can vary based on the specific flooding application of the models being trained, we report here an example workflow of training ML models for flood extent mapping from a discussion with our expert collaborators.

Data acquisition and pre-processing: The process begins with data collection, acquiring aerial imagery taken during a flood disaster with corresponding digital elevation model (DEM) data. This imagery can be obtained from a source such as NOAA’s National Geodetic Survey of Emergency Response Imagery [47] in the form of patches with global Coordinate Reference System (CRS) info. These patches are then stitched together into test regions by loading them into QGIS [50], finding which patches are needed to create a test region using their CRS info, and then using the GDAL [23] library in Python to combine them into one image. DEM data can then be created for that region in the same way by downloading and stitching together data patches at corresponding CRS values, with DEM data widely available for locations in the US [25] and globally [1]. Afterward, both imagery and DEM data need to be resampled into the same spatial resolution so that the pixels are perfectly aligned.

Image annotation, model training, and inferencing: The next step is to annotate the flooded and dry areas in the imagery to obtain ground truth labels for dependent model training and performance evaluation. Study areas for flood mapping can easily have millions of pixels, so while this can be done with semi-automatic or manual tools, it is still the most time-consuming part of the flood extent mapping process, taking multiple hours per region. Once the annotation is complete, the labeled data can be used to train deep learning models for flood detection tasks such as segmenting new data into flooded and dry regions. In order to create ML models that can robustly detect flooding on unseen data, large training sets are required. While existing work has explored using fully automated methods for creating labeled flood datasets [7], they are not widely used in practice because of quality concerns and the added difficulty for researchers to understand and explain model behavior. In our collaborators’ lab, the bulk of annotation is accomplished by trained graduate students. In our work, we hope to improve the workflows of ML researchers by reducing the burden of annotation through efficient semi-automatic tools and enabling crowdsourcing.

2.2 Crowdsourcing for Research

Nowadays, many projects (e.g. eBird [66], GalaxyZoo [43]) have shown that crowdsourcing and citizen science can be successful for large-scale data collection and annotation. Because any barrier to entry will lower the number of users of a platform, crowdsourcing applications are almost always web-based for ease of access. To define the qualities of successful crowdsourcing projects, Law et al. [41] deduced a set of requirements that make crowdsourcing feasible, desirable, and useful for a given research problem. Flood extent mapping satisfies their challenges of data sensitivity, quantity, and availability, along with crowd interest, intention, and ability as proven by other applications around crowdsourced flood event data [48,57,58]. In addition, previous work [42] has shown that, while individual crowdworkers may not perform well in flood mapping, aggregating annotations can lead to high-quality results. This work aggregates user annotations by labeling patches as flooded or dry if the ratio of received labels for that patch is above an empirically chosen certainty threshold. FloodTrace is unique in providing a system for interactively visualizing aggregated annotations with the uncertainty between annotators, which allows experts to quickly revise and improve the set of annotations.

2.3 Annotation Tools

Multiple web-based libraries such as OpenStreetMap [27], QGIS Cloud [50], and ArcGIS Online [3] provide tools for geospatial data. Each of these tools was made for different use cases but can support DEM data, interactive 3D rendering, and basic annotation with text, polygons, and brushes. Their potential for flood extent mapping, however, is limited by the fact that none provide semi-automatic annotation tools for the purpose. Even with crowdsourcing, manual annotation of flooded imagery with polygon selections and brushes is too time-consuming to be desirable and results in less accurate training data.

For semi-automatic annotation, there are two main classes of tools in this domain. The first are those that produce a segmentation of the input and allow users to apply flood or dry class labels to selected

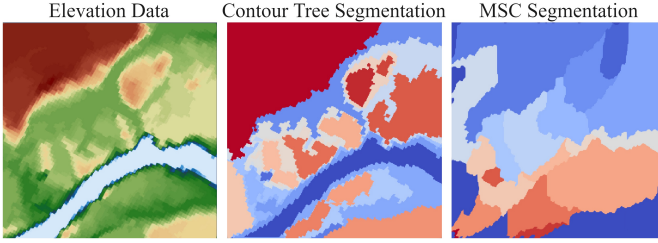


Fig. 2: Example of contour tree and Morse-Smale complex (MSC) segmentation on a 250×250 slice of DEM elevation data using the Topology Toolkit in Paraview. Before creating either segmentation, simplification by persistence was applied with a threshold of 0.1 of the function range. The contour tree segmentation shows its clear use case as a tool for selecting terrain features such as the hills and river in this example.

segments (*segmentation-type* tools). Liang et al. [42] use imagery patches exported from a graph-based clustering approach as these segments, and show that these patches can be labeled effectively by non-experts. Other work has used image features produced by class-agnostic neural networks for labeling to create large flood annotation datasets [8, 51]. The second class of tools are those where the user selects seed pixels which are then extended with connected pixels by some rule (*extension-type* tools). As an example, Gebrehiwot et al. [24] use a tool to automatically label connected pixels of the same color as flooded or dry. While the semi-automatic annotation tools mentioned so far operate directly on aerial imagery data, recent exploratory work has been done on creating an elevation-guided extension-type tool for labeling flooded datasets [2]. This work utilizes DEM data to select all connected downstream (lower elevation) or upstream (higher elevation) pixels from a selected seed pixel, which they call the breadth-first search (BFS) method. As our design seeks to enable elevation-guided annotation, we adapt their BFS method as a state-of-the-art tool in our application (Sect. 4.2.1). Still, it is important to note that the original work [2] does not support interactive 3D rendering, can only operate on small data patches, and has poor performance, all issues that are addressed by our web-based solution with GPU accelerated rendering. In addition, we develop a new elevation-guided tool that uses topological data analysis to annotate regions much more quickly than the BFS tool.

2.4 Topological Analysis of DEM Data

As the size and resolution of DEM data grow, the need for generalization and simplification of features is well known; multi-scale views are required in order to conduct meaningful analysis on DEM landforms [18, 31, 64, 65, 67]. Several methods have been proposed for this, which needed generalization and simplification of DEM data. Yu et al. [65] propose a method combining structural analysis and statistical filtering for simplification while preserving smooth morphology and structural edges. Guilbert [31] uses contours to generate a feature tree for underlying data at multiple levels of detail. Wu et al. [67] use a localized contour tree method to detect and characterize surface depressions across scales. Recently, Corcoran et al. [9] show the advantages of persistent homology methods in terrain analysis for their robustness to noise and facilitating of machine learning methods utilizing persistence diagrams as signatures of a dataset. In our work, we leverage persistent homology and contour tree methods on DEM data to enable robust annotation of features at different levels of detail.

By extracting the underlying structural information from scalar data, topological data analysis (TDA) provides many opportunities for data segmentation and simplification. Topological methods have been successfully used to extract features of interest in a variety of scientific domains [5, 6, 32, 33, 40, 49, 52, 59]. These data features can be effectively identified by using topological structures such as the Morse-Smale complex (MSC) [16] and contour trees to create segmentations of the data. The MSC does this through gradient flow, segmenting the scalar field data into regions consisting of all the paths connecting a local maximum and local minimum that follow the gradient of the scalar field. Contour trees segment data by considering contours through a sweep of

the function range, defining segments as the birth or split of a contour until it merges with another or vanishes. We provide an example of both methods of TDA segmentation on a small piece of DEM data in Fig. 2. As shown, our use case of selecting dry and flooded features correlates well with the contour tree segmentation. This method identifies terrain features such as hills and rivers, along with contours at various elevations which allow for the selection of the precise water level of a flooded area. In this work, we propose using the contour tree to create a novel segmentation-type tool for elevation-guided annotation for flood extent mapping.

One challenge is that, because DEM data is complex and large-scale, contour tree segmentations on raw data are mostly made of noisy and small segments. This, along with the necessity of identifying features at varying levels of detail, motivates our use of persistent homology for data simplification. Persistent homology [17] is a powerful tool that can be used to remove topological features that are unimportant or correspond to low-intensity noise. This is done by considering the persistence of these features, including their lifespan between birth and death when conducting a sweep through the range of the function. Simplification by persistence involves removing critical points corresponding to the birth and death of a topological feature if that feature's lifespan is below some threshold. In doing this, simplification by persistence preserves salient features in the data, in contrast to other simplification methods like downsampling the spatial resolution. As an example, a spatially small feature with a huge variance in elevation compared to its surroundings would have a large persistence value, and not be simplified until high thresholds, whereas downsampling the data's spatial resolution would remove this feature. In this way, our simplification is more robust for maintaining topological features in high-resolution data. By simplifying our data at varying persistence thresholds, we can provide effective multiscale data for selecting features in our application; this affords users the ability to quickly annotate large, obviously flooded and dry features, while maintaining the detail necessary to accurately label smaller features.

Similar topological techniques have previously been utilized for semi-automatic annotation in neuron tracing of large brain volumetric data [45]. This work utilizes the MSC to extract ridge-like structures which correspond to neuron center-lines, which can then guide user tracing. Simplification by persistence is used with an empirically chosen persistence threshold to remove noise and create a sparser dataset for users to interact with. While taking inspiration from this work, our system adapts topological methods specifically to the labeling of flood extent in terrain data. Our method of selecting contour tree segmentations that correspond to features below or above water level in terrain data is unique. Furthermore, our method of allowing interactive selection of multiscale features by providing data simplified at varying persistence thresholds is a novel technique for annotation and is necessary to find landforms at different scales within DEM data. Finally, FloodTrace is the only system the authors found that integrates topological segmentation into a web-based application for interaction.

3 DESIGN

Before implementing our solution, we conducted interviews with domain scientist collaborators (i.e., machine learning researchers building models for flood extent mapping) to understand the state-of-the-art and requirements for this project. From these discussions, we list the requirements for building an effective application for flood annotation for ML training data:

- R1: Image annotation decisions must be informed by elevation data. Elevation awareness enables robust annotation of regions that are ambiguous with only imagery data and more accurate annotation along elevation borders, naturally leading to higher quality training data for ML models that rely on elevation data. For accuracy and productivity, there should be intuitive and interactive visualization of both elevation data and flooded imagery, which is missing from previous work [2].
- R2: Annotation tools must be efficient and quick. Annotating a single flooded region usually involves labeling millions of pixels

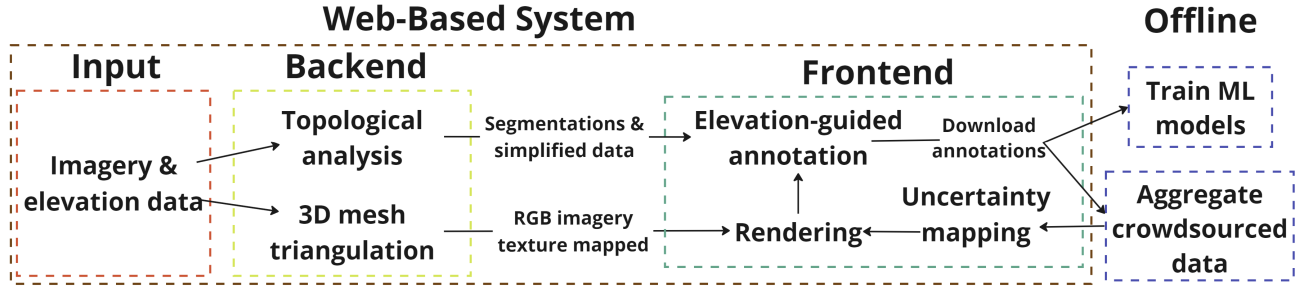


Fig. 3: An illustration of the full processing pipeline for FloodTrace.

and multiple hours of work, and study areas commonly consist of many regions. Because of this, the acquisition of ground truth labels for training is extremely time-consuming. Tools that increase annotation productivity will have a large impact on improving ML researchers' workflows.

- R3: The annotation application must fully support the large data sizes of study areas. Previous annotation work [2] can only process small patches at a time, lowering productivity and leading to potential inaccuracies on patch borders. Performance on large data should be an important aspect of the new application design.

We also discussed our collaborators' interest and concerns with crowdsourcing annotations to be used as training data. They expressed confidence that, while working on flood forecasting requires extensive experience and domain knowledge, data for flood detection (i.e. flood extent mapping) can accurately be labeled without expert knowledge by using aggregation of annotations from many participants. This is supported by previous work [42] which shows that aggregate annotation data seems to converge to the highest quality around 20-25 annotators for a particular study area, although this number likely changes depending on the difficulty of annotation region, background of participants, and tools being used. While optimistic about crowdsourcing, after discussion we were left with another requirement for our annotation system to support crowdsourcing properly:

- R4: Aggregate annotation data must be presented in an understandable way for researchers, and provide the ability to correct inaccuracies. When dependent ML models make mistakes or do not behave as intended, it is important for researchers to be able to easily check model training data for errors and remedy them, especially when relying on crowdsourced data. Our application should provide effective visualization of aggregate annotations along with tools to improve them quickly.

We implement our application to address these requirements in Sect. 4. Feedback was continuously integrated into our application throughout the implementation process, as advised by best practices [56].

4 IMPLEMENTATION

FloodTrace consists of a web-based system that addresses the requirements gathered in Sect. 3 for both crowdsourcing and direct annotation by researchers. To address R1, our system provides interactive 3D visualization of aerial imagery and DEM data (Sect. 4.1). R1 and R2 are both addressed by providing efficient elevation-guided semi-automatic annotation tools (Sect. 4.2). R4 is addressed with aggregate annotation visualization for viewing uncertainty and making corrections (Sect. 4.3). For R3, our application is built using the GPU-accelerated WebGL [28] backend in Three.js [61]. In our experimentation, the largest data size we have tested is 12000×12000 pixels, which is much larger than flood extent mapping regions. We acknowledge that limitations are present in the case that available memory will not be sufficient to host the DEM data. We give a brief overview of our UI design in Sect. 4.4.

A complete pipeline overview is given in Fig. 3. Researchers first provide corresponding aerial imagery and DEM data to the server backend for computing the 3D mesh and topological data structures

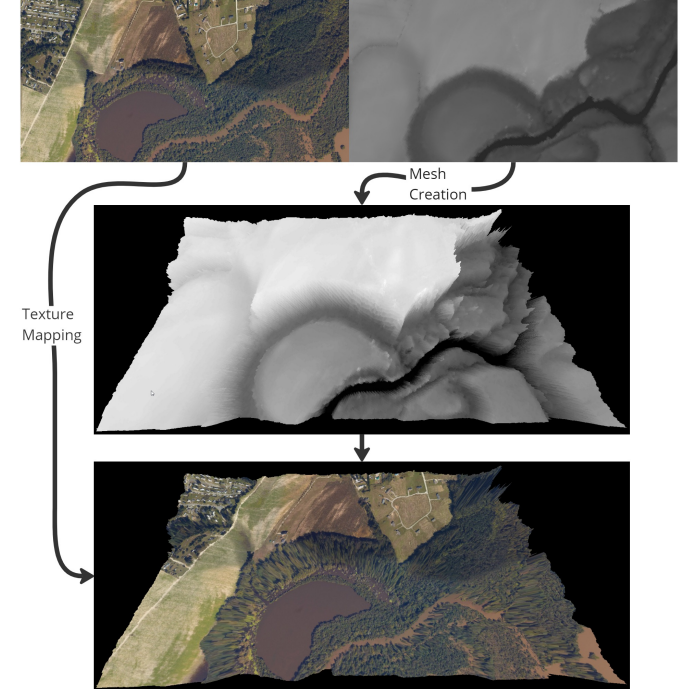


Fig. 4: An example showing mesh creation with the heightmap meshing utility and rendering with aerial imagery RGB texture on a 1000×500 resolution example.

necessary for our methods. For crowdsourcing, these can easily be pre-computed and served directly at a deployed frontend site, as in our user study ([anonymized link to demo]), removing the need for crowdworkers to be given raw data or access to the backend server. Once data is served to the frontend, annotation can be accomplished using elevation-guided annotation tools directly on an interactive 3D rendering. Once annotations are complete, they can be downloaded and, in the case of those created directly by researchers, used to train dependent ML models. In the case of crowdsourcing, annotations can be downloaded and submitted to researchers for aggregation. Researchers can then use these aggregated annotations with uncertainty visualization tools in the frontend to review and improve them before being used to train dependent ML models.

4.1 Rendering

An important feature to address R1 is providing the user with an interactive 3D visualization to inform their annotation. This is important to ensure that pixels with high or low relative elevation do not get labeled incorrectly, labels for ambiguous pixels covered by clouds or tree canopy can be inferred, and seed pixels for the BFS tool can be selected effectively.

Upon receiving the input of RGB imagery data and DEM data, mesh creation is done in the backend as shown in Fig. 3. We utilize the HMM heightmap meshing utility [19] in the backend to triangulate a mesh from the elevation image using the method of Garland and Heckbert

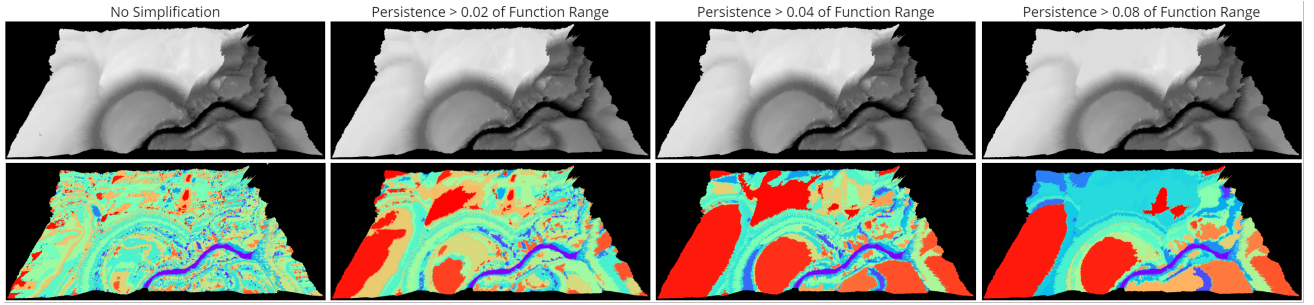


Fig. 5: An example of simplified data and resulting segmentations at persistence thresholds $\varepsilon = 0.02, 0.04$, and 0.08 of the elevation data function range. Observing the differences in elevation data that come from topological simplification is quite difficult, but the effect is clear when looking at the varying contour tree segmentations produced.

[22]. The generated STL file is sent back to the web application, where it is visualized with the RGB imagery data texture mapped onto the mesh, as shown in Fig. 4.

We acknowledge that it would be possible to render the height field directly with high accuracy in real-time [10, 15, 38], however in our initial testing, we found direct height field rendering in Three.js to impact the interactivity of our system for large datasets. Pre-computing a triangulated mesh allows for easy, interactive visualization on our front end. While triangulating a surface from DEM data has been shown to introduce more error than higher-order methods [39], we find this acceptable as the mesh itself is only used for exploration in our system, and selections for annotation by our tools are done on the full-resolution underlying data.

We initially experimented with fly-through camera controls for our rendering but decided against them after negative feedback from our collaborators. Instead, we implement orbit controls, modeling other applications that handle 3D data such as Paraview. This camera control method focuses on the annotation mesh, providing a more intuitive experience for interacting with the 3D visualization. The mouse scroll wheel controls the zoom, left click and drag rotates the camera around the mesh, and right click and drag pans the camera. In order to accommodate users working on laptops with only a trackpad who cannot right-click and drag easily, we also give an option for double-clicking on the mesh to pan to the area clicked. The camera view can be reset to its starting position with a click of a button in the menu.

To cater to the needs of our collaborators, we incorporated options that allow users to easily modify the mesh appearance and seamlessly switch between 3D and 2D views. Our collaborators expressed that having the ability to view the RGB imagery on a flat 2D mesh can be beneficial in certain situations, prompting us to include this feature. As users annotate a region, the pixels labeled as flooded or dry are overlaid with a translucent color mask of red or blue respectively. This feature can be toggled, and it is helpful to do so after annotating large features with semi-automatic tools. This allows the user to better focus on the satellite imagery underneath the annotation and ensure the area has been annotated correctly. These mesh appearance functionalities are implemented with custom WebGL fragment shaders for our ThreeJS rendering.

4.2 Elevation-Guided Annotation Tools

Following R1 and R2, FloodTrace utilizes DEM data for elevation-guided annotation tools that are able to quickly create accurate, robust labels for large flooded regions. These tools are built for intuitive use by both domain experts and crowdworkers. We provide both extension-type and segmentation-type semi-automatic methods in the form of the BFS (Sect. 4.2.1) and topological segmentation (Sect. 4.2.2) tools respectively.

4.2.1 BFS Tool

This method of extension-type semi-automatic annotation was first proposed by Adhikari et. al [2], and we adapted it as a state-of-the-art tool in our application. This tool is used by annotating a seed pixel, which is then extended in all directions by connected downstream or

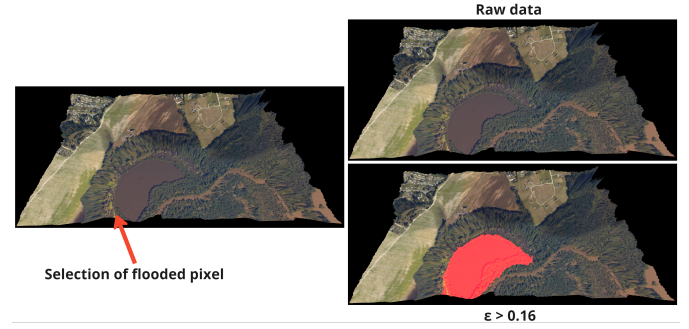


Fig. 6: An example of the selection of the same pixel as flooded with one click of the segmentation tool, first on the unsimplified elevation data and then on the data simplified with persistence threshold $\varepsilon = 0.16$. Initially, the tool labels almost no pixels, but when used at a higher simplification level it labels an entire lake feature.

upstream pixels (depending on whether the label is flooded or dry) in the DEM data. This accurately labels flooded or dry regions by taking advantage of the physical constraint that if a location is flooded, then its adjacent locations with a lower elevation will also most likely be flooded. In the same way, adjacent locations of dry areas that have higher elevations will most likely be dry. This approach accurately annotates regions along elevation border pixels, as the BFS stops where the elevation becomes higher or lower than the connected pixel, depending on if flooded or dry is being labeled. This approach also addresses the difficulty of annotating ambiguous pixels in the RGB imagery, such as those covered by tree canopy or clouds, by automatically labeling them using neighboring pixels.

Thanks to the 3D mesh rendering in FloodTrace, the user can purposefully select high-elevation flooded pixels or low-elevation dry pixels in order to label as large of a downstream or upstream area as possible, improving efficiency. Our application also provides a polygon BFS tool, where one can select points to form an arbitrary polygon, fill the polygon, and run a BFS selection from all points on the borders. This feature allows larger areas to be selected quickly while ensuring that the annotation's border pixels correctly correspond to elevation changes.

4.2.2 Topology Segmentation Tool

We provide this tool as a novel method for semi-automatic annotation of flooded regions. We utilize TDA to create a segmentation-type tool that can quickly annotate regions according to features in the elevation data. We find that contour tree segmentations give us topological features in the DEM data that correspond well to landforms such as rivers and hills (Fig. 2), with natural borders likely to correspond to flood levels.

As described in Sect. 2.4, we utilize persistent homology to simplify our data at varying thresholds before computing segmentations on these, allowing for interactive selection of features at different levels of detail. To visualize the effectiveness of simplification by persistence for contour tree segmentation, we show an example region simplified at different persistence thresholds and the corresponding segmentations

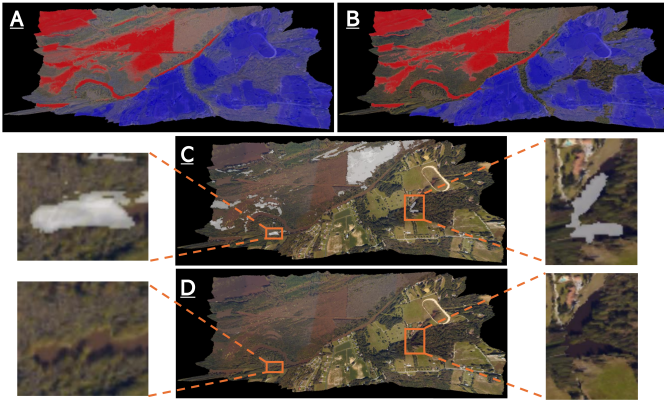


Fig. 7: Visualization of aggregated crowdsourced data from 45 participants. The aggregate view is shown in A) with no certainty threshold and in B) with a certainty threshold of 0.6. This view can quickly show the areas where the group of annotators were confident in labeling flooded or dry. The variance view is shown in C) with a threshold of 0.7 and compared in D) to a view with no annotation texture. With this view, it is easy to identify regions where there was high annotator disagreement, such as those shown in the orange borders. These selected regions are obviously flooded, and so the researcher can quickly correct these areas by labeling them. We explore how this can improve model performance in Sect. 5.

in Fig. 5. By providing all these segmentations for annotation selection, users can quickly annotate huge areas of pixels that are obviously flooded or dry while also maintaining the ability to accurately label less persistent features.

To compute segmentation and simplification in our system, FloodTrace utilizes the Python binding of the Topology Toolkit (TTK) [62], specifically its functions for simplification by persistence (which implement the works of Tierny and Pascucci [63] and Lukasczyk et al. [44]) and contour tree creation (which implement the work of Gueunet et al. [29, 30]). Given a DEM dataset, the backend computes contour tree segmentations to be used in the frontend for annotation Fig. 3. Annotation is done simply and quickly with the segmentation tool by applying flooded or dry labels to the segment currently under the cursor. The user can quickly switch between different simplification levels in the UI, interactively changing the segmentations that will be used for selection to that persistence threshold. We show example tool usage in Fig. 6, first on the raw elevation data of the region, then on the topologically simplified data at the persistence threshold 0.16 of the function range.

Based on demo feedback from our collaborators, we provide two options for visualizing the segmentations of a dataset. The first option is to paint the borders of the current segmentations on the mesh in white. This is used to quickly see which simplification level leads to the desired level of detail by viewing how segmentation borders change when cycling through the levels. The second option is to highlight in red or blue (depending on flooded or dry potential label) the segment currently hovered over by pressing the highlight key. This is used to quickly check the coverage of the selected segment to confirm it contains fully flooded or dry imagery before labeling.

To keep the interaction simple for the user study, we provided six simplification levels based on thresholds at logarithmic steps along the data’s normalized function range (i.e. $\epsilon = 0, 0.01, 0.02, 0.04, 0.08, 0.16$). In the final application, though, users can choose the number of thresholds and persistence values themselves when submitting input data, and query the backend for more simplified data as needed. Users must switch between simplification levels in order to ensure that they do not label an area so large that it includes both flooded and dry regions or so little that they do not fully capture a flooded or dry feature, so using this tool does take some user experience and experimentation.

4.3 Aggregated Annotation Visualization

In order to address R4, FloodTrace offers the capability for researchers to visualize aggregated crowdsourced annotations and fix inaccuracies before training dependent models. We accomplish this through two novel views that are inspired by work on uncertainty visualization in mapping applications. In prior work [35, 36, 55], the uncertainty of 2-dimensional variables was communicated effectively through inverse mapping of color saturation to the magnitude of uncertainty; when the value of the variable is more uncertain, the pixel’s color is made to have lower saturation. We follow this standard, with uncertainty for pixels in our aggregate visualization defined by scarcity of labels or variance between annotators’ labels in the given set of annotations.

Before visualization, each annotation in a given set is transformed into a 2-dimensional array where red (flooded) pixels are made -1, transparent (unlabeled) pixels are made 0, and blue (dry) pixels are made 1. For our first view, the aggregate view, we find the mean for each pixel across annotations, giving a value in [-1, 1] where a score of -1 means all annotators agreed the pixel is flooded, 1 means all annotators agreed the pixel is dry, and scores closer to 0 mean the annotators either disagreed or chose not to label the pixel. These values are then visualized as a color-mapped texture on the 3D rendering within our application. We follow the standard of inversely mapping uncertainty to saturation in our colormap, but, because the underlying RGB imagery also contains important information for the researcher, we extend this by additionally mapping uncertainty to texture transparency. Pixels that annotators uniformly labeled as flooded or dry are colored with a more opaque red or blue, while this color becomes more white and transparent the more uncertain annotators were about its label. To simplify the texture being mapped, a sliding tool in our interaction menu gives users the ability to threshold pixels by their certainty, collapsing values to 0 if their absolute value is not greater than the threshold. As 0 corresponds to full transparency in our colormap, this effectively hides the value of pixels below the threshold. An example of this view aggregated from 45 unique annotations from our user study is shown in Fig. 7 (A, B). This view was developed with collaborator feedback as a way to quickly understand the labels being used for training data and identify possible sources of error, helping to address R4. In addition, while dependent models can be trained using soft labels of flood and dry scores, the ability to explore certainty thresholds in our view allows researchers to find effective values for binarizing aggregate data into hard labels.

In order to fully address R4, we create another view specifically for correcting aggregate annotations. This view, the variance view, highlights the areas where annotators disagreed the most, as these are likely to be inaccurately annotated. While the first view displays the mean pixel values for a set of annotations, this one displays the variance. We use a similar color mapping as before, with higher uncertainty (in this case variance) corresponding to whiter color, but because we want to focus the user on the areas of high uncertainty for correction, we inversely map uncertainty to texture transparency. This view is shown in Fig. 7 (C). With this view, researchers can easily check the areas of high variance and correct them with our annotation tools if they find them obviously flooded or dry. The crowdsourced annotations can then be downloaded with the corrected areas labeled for more accurate model training. With these two views, we enable ML researchers to rely on crowdsourced annotation data by making the aggregated data understandable and easily fixable when errors occur.

4.4 User Interaction

The UI for FloodTrace is shown in Fig. 8, with an interaction menu in the top right, toggles between erase/fill and flood/dry selection in the top left, key reminders in the bottom left, and checkpoint/finish buttons in the bottom right. The on-screen UI is limited in order to simplify user experience and allow the annotation mesh to take up the full view. Along with the semi-automatic tools, we also provide a brush to manually annotate if desired, such as to erase unwanted annotation.

Users make annotations by aiming the mouse cursor at an area of the mesh and pressing the chosen key of any of the annotation tools. Point BFS, segmentation, and brush tools immediately annotate the

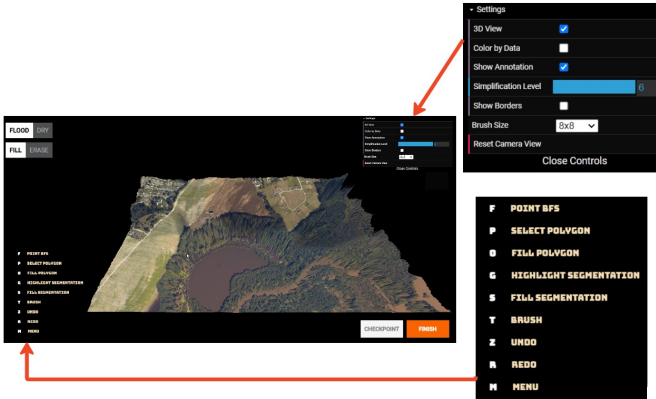


Fig. 8: UI for our application. Options and key reminders are blown up for visibility. Note the minimal screen space taken up by UI components so that the region being annotated can make use of the full screen.

area underneath the cursor using their respective algorithms (with the brush simply painting a square) on key press. Polygon selection with BFS, however, occurs by pressing a key to repeatedly select desired points on the polygon to be drawn and then pressing another key to confirm the selection which then runs the BFS method to fill the pixels within that polygon and surroundings.

Annotation tools apply color to the annotation texture determined by whether one is annotating as dry (blue) or flooded (red). The current annotation type is toggled with a switch on the top left of the UI and it also affects whether the BFS method selects upstream or downstream pixels. Users can also toggle annotation mode from 'Fill' to 'Erase' in order to use all the different annotation tools to remove annotation color rather than paint on the texture. Undo and redo functionality are given to allow users to take back accidental or ill-thought-out annotations, and put them back again.

As users utilize the various tools in FloodTrace, all of their actions are logged with enough detail to replay their session completely given an output log. This gives the ability to create checkpoints during annotation, where the state of the current session is downloaded as a JSON log file and can be uploaded in the future to restart the session at that state. Sessions can also be started with a given annotation texture. When a user selects to finish their session, their log file, annotation texture, and metadata about the session are downloaded.

5 EVALUATION

In this evaluation, we study how FloodTrace is able to enable crowdsourced annotation through an experimental user study. The setup of this study is explained in Sect. 5.1. We use the results of this study to assess the efficiency of our semi-automatic tools, how the insight given by these and 3D rendering affect annotation accuracy, and the value of our aggregate visualization and correction strategy. To do this, we first analyze the accuracy and annotation speed of participants (Sect. 5.2). We then use participant annotations as training data for flood detection models and assess model quality (Sect. 5.3).

5.1 User Study Setup

The dataset used for annotation for the study consists of flooded regions of North Carolina during Hurricane Matthew in 2016, with high-resolution aerial imagery from the National Oceanic and Atmospheric Administration National Geodetic Survey [47] and corresponding DEM data from the University of North Carolina Libraries [12]. All data was resampled to a resolution of 2 square meters per pixel, which is common in this domain [37, 53, 68]. Eight separate regions were chosen with dimensions between 4104×1856 pixels and 6472×3136 pixels, and these regions were split into quadrants for smaller workloads for participants of the study.

297 graduate students of a machine learning course volunteered to participate in this study, of which 266 followed through with final submissions. Before beginning annotation work, participants watched

an instructional video explaining how to use all of the features of FloodTrace and how to determine whether to mark areas as dry or flooded. They were then given access to a web application which they could visit at any time within the following two weeks to complete the work assigned to them. On the application, all interactions made by the students were logged, and these logs were submitted along with output annotations on completion. Each student was asked to complete five annotation tasks, with each task requiring annotating at least 60% of a quadrant of one of our chosen regions as flooded or dry, leaving any remaining pixels as unlabeled. These tasks were created for two specific experiments, in addition to providing a reasonable number of annotations and interaction logs to draw insight from.

The goal of the first experiment was to fairly compare the effectiveness of the annotation tools, ensuring that participants became familiar with both semi-automatic tools. This experiment consisted of three annotation tasks performed on the same quadrant. For the first, the user would perform annotation while restricted to only one of the semi-automatic tools. Next, they would complete the same annotation task while restricted to the semi-automatic tool they did not have in the first task. Last, they would complete the annotation task again with access to both semi-automatic tools. Participants were divided evenly so that half started with the BFS tool and half started with the segmentation tool. Brush tools were provided in all three tasks to allow students to make fine-grained corrections or label features that were difficult to annotate semi-automatically.

The second experiment was meant to test the effectiveness of the 3D mesh in improving participants' insight and accuracy. This required users to perform two annotation tasks on the same quadrant, although a different one than used in the first three tasks. First, they would annotate the quadrant while restricted to only a 2D view of the aerial imagery, then they would annotate the same quadrant with the 3D mesh and full 3D view interactivity. Both tasks for this experiment had full access to brush and semi-automatic tools.

At the conclusion of this study, we received 266 submissions, with 259 of those including all five tasks that the participant was assigned. Aggregating all submissions, each quadrant in our dataset was annotated on average 41 times, 1,321 total annotations were collected, and participants collectively annotated over 3.5 billion pixels. We open source this dataset of annotations as a contribution of this paper, along with metadata for each annotation.

5.2 User Study Analysis

Because the goals of R1 and R2 are to increase annotation speed and accuracy, these are the metrics we study. We measure annotation speed simply as the time taken to complete an annotation. We measure annotation accuracy by comparing participant annotations against reference annotations that were manually labeled either by our domain expert collaborators, or members of our team after being trained. To avoid penalizing unlabeled pixels, we only consider pixels that were labeled as flooded or dry in both the participant and the reference annotation when measuring accuracy. The formula we use to compute accuracy is shown below where TF and TD are true flooded and true dry (pixels with the same label in participant and reference), and FF and FD are false flooded and false dry (pixels with opposite labels in participant and reference):

$$\frac{TF + TD}{TF + TD + FF + FD} \times 100\%$$

An accuracy percentage of 0% here means all participant-labeled pixels disagreed with all corresponding labels in the reference, 100% means all user-labeled pixels agreed with corresponding labels in the reference, and 50% means half of the user-labeled pixels agreed with corresponding labels in the reference. Note a score of 50% can be achieved by labeling pixels completely randomly since there is a 50% chance of guessing a flooded or dry label correctly.

Impact of Annotation Tools In order to study how the usage of different tools affected these metrics, we grouped annotations by their tool usage using the activity logs submitted with participants' annotations. Before analysis, we first conducted data cleaning to remove

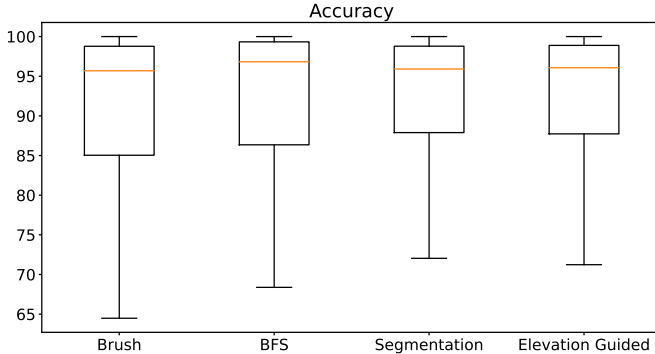


Fig. 9: Box and whisker plot showing the accuracy of the brush, BFS, segmentation, and elevation guided groups.

potential spoilers from the dataset, as we found some participants to misunderstand the labeling task or leave the application open without progress for extremely long periods. We computed the means and standard deviations for annotation completion time and accuracy, and used these to compute a threshold at which to discard annotations. We chose a standard z-score of 3 as our cutoff point (meaning 3 standard deviations from the mean, or falling outside of the 99.7% confidence interval), and were left with thresholds of 17.6 hours for annotation time and 55.4% for accuracy. Because the variance of annotation times was much higher than the variance of accuracies, the time threshold could likely be more aggressive; the median completion time was only 32 minutes, so it seems probable that times above a few hours would be the result of idling on the page. We investigated using z-scores of 1 and 2 to create stricter time thresholds (corresponding to 7.0 and 12.3 hours respectively), but found that these led to the same statistically significant conclusions as using a z-score of 3, only more pronounced, so we present here the results using the more inclusive 17.6 hour cutoff. With our time and accuracy thresholds, we discard a total of 40 annotations and leave 1,281 activity logs for analysis. Using these, we create four groups based on tool usage as described below:

Brush: Annotations where the brush tool was used to label > 50% of all labeled pixels

BFS: Annotations where the BFS tools (polygon and point selection) were used to label > 50% of all labeled pixels

Segmentation: Annotations where the segmentation tool was used to label > 50% of all labeled pixels

Elevation Guided: Annotations where elevation-guided tools (segmentation and both BFS selections) combined were used to label > 50% of all labeled pixels

In order, these groups ended up with sizes of 787, 134, 346, and 494 annotations. We find that, even though the instructional video emphasized that participants should rely mostly on the elevation-guided tools, users gravitated more towards the more simple and familiar brush tool. This likely shows an example of algorithm aversion [13, 14], where users are proven to prefer human decision-making rather than algorithmic tools even when presented with algorithms that outperform humans. We acknowledge that this could be fixed in future deployments by forcing some usage of the elevation-guided tools before the brush tool is unlocked, but we leave more in-depth approaches to overcoming algorithm aversion as future work.

We present annotation accuracy results for these groups in a box and whisker plot in Fig. 9. We provide the mean accuracies in Table 1, along with Welch's t-test results to test for statistical significance in difference against the brush group. From these results, we find that those who relied on elevation-guided tools were able to produce more accurate annotations than those who relied on the brush tool, which is guided solely by user insight. This shows that both elevation-guided tools are effective for improving accuracy (and thus training

| | Brush | BFS | Segmentation | Elevation Guided |
|------------------|-------|-------|--------------|------------------|
| Mean | 90.52 | 91.76 | 91.64 | 91.67 |
| P-Value vs Brush | - | 0.092 | 0.031 | 0.020 |

Table 1: Mean accuracies and p-values from t-tests against the brush group. We find all three groups that rely on elevation-guided tools to be more accurate than the group using the manual tool. All comparisons are statistically significant except the BFS group, likely because the group had a much smaller sample size.

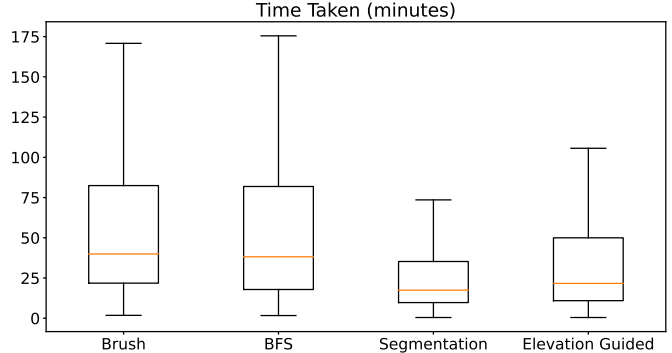


Fig. 10: Box and whisker plot showing the time taken for annotations in the brush, BFS, segmentation, and elevation guided groups. We find use of the segmentation tool to drastically reduce the time taken to complete an annotation, with brush and BFS groups having median times of 39.97 and 38.18 minutes while segmentation and elevation-guided groups took only 17.45 and 21.65 minutes.

data quality), even for untrained crowdworkers. We additionally ran t-tests for the differences between the BFS, segmentation, and elevation-guided groups, but found no statistically significant outcomes.

We present annotation speed results in a box and whisker plot in Fig. 10. This plot shows that annotations relying on the segmentation tool were much faster than those that did not, with the median time taken of the segmentation group being $2.29 \times$ and $2.19 \times$ smaller than the medians of the brush and BFS groups respectively. We ran t-tests again to measure the significance of the differences in time taken between groups, and found the differences between segmentation and brush, segmentation and bfs, and elevation-guided and brush to be significant with p-values < 0.00 , with other group differences not significant except elevation-guided and BFS at 0.036. These results clearly support our segmentation tool as a method of quick annotation while preserving high accuracy, and show it outperforms the BFS tool in efficiency. Importantly, these results show that even untrained crowdworkers can use this tool effectively.

To further explore how the annotation tools affect accuracy and speed, we additionally compute the Pearson correlation coefficient r between each tool's usage and our metrics. Tool usage is computed as the ratio of the number of pixels annotated by a tool divided by the total pixels labeled in that annotation. This data is presented in Table 2. The correlation coefficient r is measured in $[-1, 1]$ where -1 is the strongest negative correlation, 1 is the strongest positive correlation, and 0 is no correlation.

Results show that the segmentation tool has a strong negative correlation with time taken, while brush had a strong positive correlation

| Tool | Time Taken | | Accuracy | |
|--------------|------------|---------|----------|---------|
| | r | P-Value | r | P-Value |
| BFS | 0.022 | 0.218 | 0.053 | 0.029 |
| Segmentation | -0.137 | 0.000 | 0.034 | 0.114 |
| Brush | 0.111 | 0.000 | -0.065 | 0.010 |

Table 2: Pearson correlation coefficients r and p-values for relationships between tool usage and our accuracy and speed metrics. P-values under 0.05 indicate statistical significance. Coefficients close to 0 indicate no correlation, while values closer to 1 and -1 indicate positive and negative correlations. All correlations are significant except time taken with BFS tool and accuracy with segmentation tool.

and BFS had no significant correlation. This shows that the more a participant used the segmentation tool, the faster they were able to complete their annotation. With regards to accuracy, usage of the BFS tool correlated with higher accuracy, meaning increased usage led to increased accuracy in the resulting annotation, and opposite for the brush tool. The correlation with accuracy was also positive for the segmentation tool, but it was smaller and not statistically significant. This shows that, while annotations that utilized the segmentation tool were accurate (i.e. those in the segmentation group), increasing usage of the tool did not always mean increased accuracy. Although the segmentation tool is the quickest way to annotate accurately, annotations are most accurate when it is supplemented with the BFS or brush tools to fill in gaps and make small corrections.

Impact of 3D View We also assess how providing users with a 3D rendering affects their accuracy, using the two annotation tasks from the second experiment in Sect. 5.1. As a note, participants' accuracy in these tasks was higher than the overall average, stemming from the fact that participants completed these annotation tasks last, and their accuracy with the tools improved through learning over time. For this experiment we form two groups, flat, consisting of the annotation tasks restricted to the flat view, and 3D, consisting of the subsequent annotation tasks with access to the 3D rendering. Using the same accuracy and time thresholds as above, we get groups of 262 and 250 annotations for flat and 3D respectively. The mean accuracies for flat and 3D were 91.90 and 92.94, and the p-value for the t-test between them was 0.094, which is not significant at a 95% confidence interval. We hypothesize that the difference in accuracy was narrowed by the use of elevation-guided tools, which were able to compensate for the insight lost from not being able to view the 3D rendering. We tested this by rerunning the analysis while restricting the flat and 3D groups to only include annotations in the brush group. These new flat and 3D groups included 150 and 144 annotations respectively, had means of 90.96 and 92.69, and the p-value computed between the difference in their accuracies was 0.058. While these results are still not significant, the difference in accuracy did become larger, and the p-value lower. In the future, we hope that extending this experiment with a larger sample size could lead to more conclusive results.

5.3 Crowdsourced Annotations for ML Model Training

In this section, we show how FloodTrace can enable researchers to use crowdsourced annotations as high-quality training data through an aggregation and correction process, which we detail in Sect. 5.3.1. We propose this step to replace the extremely time-consuming annotation step of researchers' workflows. To assess the training data quality of the results from aggregation and correction, we use study participants' annotations as training data for deep learning models and compare them against models trained with reference annotations Sect. 5.3.2.

5.3.1 Example Aggregation and Correction

As detailed in Sect. 4.3, our system offers the capability to visualize aggregated crowdsourced annotations and fix inaccuracies. We conducted an example for this on two randomly selected regions, collecting all the annotations for those regions from our user study. We purposefully did not use any accuracy, time, or tool usage cutoffs when creating these sets of annotations in order to ensure there would be inaccuracies in the aggregate data. For each region, there was an average of 45 annotations per pixel. We input these sets to the application frontend, and one of our trained users utilized our aggregate and uncertainty views to correct each region. On average, 4% of each region's pixels were corrected. This process was timed, and it took an average of 24 minutes to make each region's correction annotation. We compare this to the average time it took our trained users to create reference annotations in our application, which was 116 minutes per region. As training robust flood detection models requires many different annotated regions, this demonstrates how the crowdsourcing and correction workflow can save researchers huge amounts of time compared to the typical annotation process.

| Group | Class | Precision | Recall | F | Avg. F | Accuracy |
|-------------|-------|-----------|--------|-------|--------|----------|
| Uncorrected | Dry | 0.902 | 0.959 | 0.930 | 0.895 | 90.6% |
| | Flood | 0.916 | 0.810 | 0.859 | | |
| Corrected | Dry | 0.973 | 0.947 | 0.960 | 0.934 | 94.4% |
| | Flood | 0.881 | 0.937 | 0.908 | | |
| Reference | Dry | 0.963 | 0.952 | 0.957 | 0.933 | 94.2% |
| | Flood | 0.897 | 0.919 | 0.908 | | |

Table 3: Performance metrics for models trained using uncorrected, corrected, and reference labels as ground truths.

5.3.2 Prediction Setup and Results

In order to use our crowdsourced annotations (corrected and uncorrected) to train our models, we preprocess them by turning each group of annotations into a training set of soft labels. This is done by computing the flood and dry scores for each pixel, where the flood score is the sum of the number of times it was annotated as flooded divided by the number of times it was annotated as either flooded or dry, with dry scores using the same formula. We ignore unlabeled pixels in each annotation to compute these scores.

For our deep learning models, we follow the architecture described by Adhikari et al. [2] to create elevation-aware U-Net classification models to predict flooded and dry labels. Resulting predictions from this architecture take the form of a probability map, where pixels in the input are predicted with both flooded and dry probability values. We transform this into a binary class format for evaluation metrics by choosing the higher of the two scores for each pixel and applying that label. This gives us a fully labeled output, which we compare with our reference annotations to compute precision, recall, and f-scores for each class, along with accuracy as computed before. As the reference annotations include some unlabeled pixels, we ignore model predictions for these when computing metrics.

We initialized three models, using the architecture described, and trained each of them in the same two regions. Each model used a different set of labels as its respective ground truths during training, with one model using the uncorrected crowdsourced labels, one using the corrected crowdsourced labels, and one using our reference labels. We then use these three trained models to predict flooded and dry labels for an unseen test region and compute quality metrics by comparing them with the reference annotation for that region. We show these results for each group in Table 3. We find that, with the corrected crowdsourced labels, we are able to achieve around equal results (measured in accuracy and f-score) to our expert-labeled references and improve dramatically over the uncorrected labels.

6 CONCLUSION AND LIMITATIONS

We have proposed FloodTrace, a novel web-based framework for quick and accurate annotation of flooded regions that better enables crowdsourcing. This framework was built directly from requirements gathered from researchers in flood extent mapping, and incorporated their feedback continuously through development. Our application utilizes a region's DEM elevation data to provide users insight in 3D and guide users with semi-automatic annotation tools, improving their accuracy. This application has already been utilized for the creation of training data by domain experts for cutting-edge flood extent mapping models [54]. The application includes a novel annotation method that uses topological data analysis to greatly outperform the state-of-the-art elevation-guided tool in efficiency. Our experimental user study shows that the benefits of our tools can be found even for untrained users. With our method for aggregating and correcting groups of annotations, researchers are able to use crowdsourced annotations as training data with equal performance to fully expert-labeled data. This improves their workflows greatly, replacing an extremely time-consuming annotation process with a much quicker aggregation and correction step.

Our work is not without limitations, though. For example, our work only supports labeling for two classes of pixels, flooded or dry. Selecting features of the data with more specific labels, such as permanent water bodies, is useful for some flood detection models. Future work could tackle extending elevation-guided tools to annotation tasks with more informative labels than simply flooded or dry. There are also

limitations with regards to the use of DEM data. As with the machine learning algorithms that rely on DEM data, our system requires that the DEM data and flooded aerial imagery are collected at similar dates. If not, deviations between elevation at the time of flooding and time of DEM collection could lead to annotation error. In addition, it is required that the DEM data precisely matches the region of aerial imagery being annotated, which necessitates pre-processing by the researcher. For the study discussed, we downsampled DEM data to match the spatial resolution of the aerial imagery, and have not investigated the effect of using DEM data and aerial imagery with differing resolutions, which could lead to conflict in annotation. Last, the use of DEM data means that objects above the ground level are absent. This is important for labeling areas with tree canopies and buildings, as we wish to consider them flooded if the ground level is flooded. However, for some regions, such as heavily urban environments with many buildings, the presence of these objects could affect water propagation enough to cause the semi-automatic tools to label things incorrectly, for example causing the BFS to falsely label downstream pixels as flooded when the water actually stopped at a building. In the future, it would be interesting to consider semi-automatic tools that utilize digital surface model (DSM) data, taking into account above-ground structures, for use cases on more urban regions.

REFERENCES

- [1] M. Abrams, R. Crippen, and H. Fujisada. ASTER global digital elevation model (GDEM) and ASTER global water body dataset (ASTWBD). *Remote Sensing*, 12(7), 2020. doi: 10.3390/rs12071156
- [2] S. Adhikari, D. Yan, M. T. Sami, J. Khalil, L. Yuan, B. R. Joy, Z. Jiang, and A. M. Sainju. An elevation-guided annotation tool for flood extent mapping on earth imagery (demo paper). In *Proceedings of the 30th International Conference on Advances in Geographic Information Systems, SIGSPATIAL '22*. Association for Computing Machinery, New York, NY, USA, 2022. doi: 10.1145/3557915.3560962
- [3] ArcGIS Online. <https://www.arcgis.com/index.html>.
- [4] R. Bentivoglio, E. Isufi, S. N. Jonkman, and R. Taormina. Deep learning methods for flood mapping: a review of existing applications and future research directions. *Hydrology and Earth System Sciences*, 26(16):4345–4378, 2022. doi: 10.5194/hess-26-4345-2022
- [5] H. Bhatia, A. G. Gyulassy, V. Lordi, J. E. Pask, V. Pascucci, and P.-T. Bremer. TopoMS: Comprehensive topological exploration for molecular and condensed-matter systems. *Journal of Computational Chemistry*, 39(16):936–952, 2018. doi: 10.1002/jcc.25181
- [6] A. Bock, H. Doraiswamy, A. Summers, and C. Silva. Topoangler: Interactive topology-based extraction of fishes. *IEEE Transactions on Visualization and Computer Graphics*, 24(1):812–821, 2018. doi: 10.1109/TVCG.2017.2743980
- [7] D. Bonafilia, B. Tellman, T. Anderson, and E. Issenberg. Sen1floods11: a georeferenced dataset to train and test deep learning flood algorithms for Sentinel-1. In *2020 IEEE/CVF Conference on Computer Vision and Pattern Recognition Workshops (CVPRW)*, pp. 835–845, 2020. doi: 10.1109/CVPRW50498.2020.00113
- [8] T. Chowdhury, R. Murphy, and M. Rahemoonfar. RescueNet: A High Resolution UAV Semantic Segmentation Benchmark Dataset for Natural Disaster Damage Assessment. *arXiv e-prints*, p. arXiv:2202.12361, Feb, 2022. doi: 10.48550/arXiv.2202.12361
- [9] P. Corcoran and C. B. Jones. Topological data analysis for geographical information science using persistent homology. *International Journal of Geographical Information Science*, 37(3):712–745, 2023. doi: 10.1080/13658816.2022.2155654
- [10] D. Cornel, S. Zechmeister, E. Gröller, and J. Waser. Watertight incremental heightfield tessellation. *IEEE Transactions on Visualization and Computer Graphics*, 29(9):3888–3899, 2023. doi: 10.1109/TVCG.2022.3173081
- [11] L. C. Degrossi, J. P. de Albuquerque, M. C. Fava, and E. M. Mendiondo. Flood citizen observatory: a crowdsourcing-based approach for flood risk management in brazil. In *SEKE*, pp. 570–575, 2014.
- [12] LIDAR Based Elevation Data for North Carolina. <https://www.lib.ncsu.edu/gis/elevation#lidar>.
- [13] B. Dietvorst. People reject (superior) algorithms because they compare them to counter-normative reference points. *SSRN Electronic Journal*, 01 2016. doi: 10.2139/ssrn.2881503
- [14] B. J. Dietvorst, J. P. Simmons, and C. Massey. Algorithm aversion: people erroneously avoid algorithms after seeing them err. *J Exp Psychol Gen*, 144(1):114–126, Nov. 2014. doi: 10.1037/xge0000033
- [15] J. Dupuy. Concurrent binary trees (with application to longest edge bisection). *Proc. ACM Comput. Graph. Interact. Tech.*, 3(2), aug 2020. doi: 10.1145/3406186
- [16] H. Edelsbrunner, J. Harer, V. Natarajan, and V. Pascucci. Morse-Smale complexes for piecewise linear 3-manifolds. In *Proceedings of the Nineteenth Annual Symposium on Computational Geometry, SCG '03*, p. 361–370. Association for Computing Machinery, New York, NY, USA, 2003. doi: 10.1145/777792.777846
- [17] H. Edelsbrunner, D. Letscher, and A. Zomorodian. Topological persistence and simplification. In *Proceedings of the 41st Annual Symposium on Foundations of Computer Science*, pp. 454–463, 2000. doi: 10.1109/SFCS.2000.892133
- [18] R. Feciskanin and J. Minár. Polygonal simplification and its use in DEM generalization for land surface segmentation. *Transactions in GIS*, 25(5):2361–2375, 2021. doi: 10.1111/tgis.12796
- [19] M. Fogelman. Heightmap Meshing Utility. <https://github.com/fogelman/hmm>.
- [20] U. N. O. for Disaster Risk Reduction. *Global Assessment Report on Disaster Risk Reduction 2022*. United Nations, 2022 ed., 2022. doi: 10.18356/9789210015059
- [21] H. Gao, G. Barbier, and R. Goolsby. Harnessing the crowdsourcing power of social media for disaster relief. *IEEE Intelligent Systems*, 26(3):10–14, 2011. doi: 10.1109/MIS.2011.52
- [22] M. Garland and P. S. Heckbert. Fast polygonal approximation of terrains and height fields. Technical Report CMU-CS-95-181, School of Computer Science, Carnegie Mellon University, Pittsburgh, Pennsylvania, 1995.
- [23] GDAL/OGR contributors. *GDAL/OGR Geospatial Data Abstraction software Library*. Open Source Geospatial Foundation, 2024. doi: 10.5281/zenodo.5884351
- [24] A. Gebrehiwot, L. Hashemi-Beni, G. Thompson, P. Kordjamshidi, and T. E. Langan. Deep convolutional neural network for flood extent mapping using unmanned aerial vehicles data. *Sensors*, 19(7), 2019. doi: 10.3390/s19071486
- [25] D. B. Gesch, G. A. Evans, M. J. Oimoen, and S. Arundel. *The National Elevation Dataset*, pp. 83–110. American Society for Photogrammetry and Remote Sensing, 2018.
- [26] M. F. Goodchild and J. A. Glennon. Crowdsourcing geographic information for disaster response: a research frontier. *International Journal of Digital Earth*, 3(3):231–241, 2010. doi: 10.1080/17538941003759255
- [27] A. Y. Grinberger, M. Minghini, L. Juhász, G. Yeboah, and P. Mooney. OSM science—the academic study of the OpenStreetMap project, data, contributors, community, and applications. *ISPRS International Journal of Geo-Information*, 11(4):230, 2022. doi: 10.3390/ijgi11040230
- [28] K. Group. WebGL: LOW-LEVEL 3D GRAPHICS API BASED ON OPENGL ES. <https://www.khronos.org/api/webgl>, 2024. [Online; accessed 11-March-2024].
- [29] C. Gueunet, P. Fortin, J. Jomier, and J. Tierny. Task-based augmented merge trees with fibonacci heaps. In *2017 IEEE 7th Symposium on Large Data Analysis and Visualization (LDAV)*, pp. 6–15, 2017. doi: 10.1109/LDAV.2017.8231846
- [30] C. Gueunet, P. Fortin, J. Jomier, and J. Tierny. Task-based augmented contour trees with Fibonacci heaps. *IEEE Transactions on Parallel and Distributed Systems*, 30(8):1889–1905, 2019. doi: 10.1109/TPDS.2019.2898436
- [31] E. Guillet. Multi-level representation of terrain features on a contour map. *GeoInformatica*, 17, 04 2013. doi: 10.1007/s10707-012-0153-z
- [32] A. Gyulassy, M. Duchaineau, V. Natarajan, V. Pascucci, E. Bringa, A. Higginbotham, and B. Hamann. Topologically clean distance fields. *IEEE Transactions on Visualization and Computer Graphics*, 13(6):1432–1439, 2007. doi: 10.1109/TVCG.2007.70603
- [33] A. Gyulassy, A. Knoll, K. C. Lau, B. Wang, P.-T. Bremer, M. E. Papka, L. A. Curtiss, and V. Pascucci. Interstitial and interlayer ion diffusion geometry extraction in graphitic nanosphere battery materials. *IEEE Transactions on Visualization and Computer Graphics*, 22(1):916–925, 2016. doi: 10.1109/TVCG.2015.2467432
- [34] L. Hashemi-Beni and A. A. Gebrehiwot. Flood extent mapping: An integrated method using deep learning and region growing using UAV optical data. *IEEE Journal of Selected Topics in Applied Earth Observations and Remote Sensing*, 14:2127–2135, 2021. doi: 10.1109/JSTARS.2021.3051873

[35] T. Hengl. Visualisation of uncertainty using the hsi colour model: Computations with colours. *Proceedings of the 7th International Conference on GeoComputation*, pp. 1–12, 2003.

[36] T. Hengl and N. Toomanian. Maps are not what they seem: representing uncertainty in soil-property maps. *Proc. Accuracy*, pp. 805–813, 01 2006.

[37] Z. Jiang and A. M. Sainju. Hidden Markov contour tree: A spatial structured model for hydrological applications. In *Proceedings of the 25th ACM SIGKDD International Conference on Knowledge Discovery and Data Mining*, KDD '19, p. 804–813. Association for Computing Machinery, New York, NY, USA, 2019. doi: 10.1145/3292500.3330878

[38] B. Kerbl, L. Horváth, D. Cornel, and M. Wimmer. An Improved Triangle Encoding Scheme for Cached Tessellation. In N. Pelechano and D. Vanderhaeghe, eds., *Eurographics 2022 - Short Papers*. The Eurographics Association, 2022. doi: 10.2312/egs.20221031

[39] D. B. Kidner. Higher-order interpolation of regular grid digital elevation models. *International Journal of Remote Sensing*, 24(14):2981–2987, 2003. doi: 10.1080/0143116031000086835

[40] D. Laney, P. Bremer, P. Miller, V. Pascucci, and A. Mascarenhas. Understanding the structure of the turbulent mixing layer in hydrodynamic instabilities. *IEEE Transactions on Visualization and Computer Graphics*, 12(05):1053–1060, Sep 2006. doi: 10.1109/TVCG.2006.186

[41] E. Law, K. Z. Gajos, A. Wiggins, M. L. Gray, and A. Williams. Crowdsourcing as a tool for research: Implications of uncertainty. In *Proceedings of the 2017 ACM Conference on Computer Supported Cooperative Work and Social Computing*, CSCW '17, pp. 1544–1561. ACM, New York, NY, USA, 2017. doi: 10.1145/2998181.2998197

[42] J. Liang, P. Jacobs, and S. Parthasarathy. Human-guided flood mapping: From experts to the crowd. In *Companion Proceedings of the The Web Conference 2018*, WWW '18, p. 291–298. International World Wide Web Conferences Steering Committee, Republic and Canton of Geneva, CHE, 2018. doi: 10.1145/3184558.3186339

[43] C. J. Lintott, K. Schawinski, A. Slosar, K. Land, S. Bamford, D. Thomas, M. J. Raddick, R. C. Nichol, A. Szalay, D. Andreescu, P. Murray, and J. Vandenberg. Galaxy Zoo: morphologies derived from visual inspection of galaxies from the Sloan Digital Sky Survey*. *Monthly Notices of the Royal Astronomical Society*, 389(3):1179–1189, 09 2008. doi: 10.1111/j.1365-2966.2008.13689.x

[44] J. Lukasczyk, C. Garth, R. Maciejewski, and J. Tierny. Localized topological simplification of scalar data. *IEEE Transactions on Visualization and Computer Graphics*, 27(2):572–582, 2021. doi: 10.1109/TVCG.2020.3030353

[45] T. McDonald, W. Usher, N. Morrical, A. Gyulassy, S. Petruzza, F. Federer, A. Angelucci, and V. Pascucci. Improving the usability of virtual reality neuron tracing with topological elements. *IEEE Transactions on Visualization and Computer Graphics*, 27(2):744–754, 2021. doi: 10.1109/TVCG.2020.3030363

[46] D. F. Muñoz, P. Muñoz, H. Moftakhari, and H. Moradkhani. From local to regional compound flood mapping with deep learning and data fusion techniques. *Science of The Total Environment*, 782:146927, 2021. doi: 10.1016/j.scitotenv.2021.146927

[47] National Geodetic Survey Emergency Response Imagery. https://geodesy.noaa.gov/storm_archive/storms/.

[48] G. Panteras and G. Cervone. Enhancing the temporal resolution of satellite-based flood extent generation using crowdsourced data for disaster monitoring. *International Journal of Remote Sensing*, 39(5):1459–1474, 2018. doi: 10.1080/01431161.2017.1400193

[49] S. Petruzza, A. Gyulassy, S. Leventhal, J. J. Baglino, M. Czabaj, A. D. Spear, and V. Pascucci. High-throughput feature extraction for measuring attributes of deforming open-cell foams. *IEEE Transactions on Visualization and Computer Graphics*, 26(1):140–150, 2020. doi: 10.1109/TVCG.2019.2934620

[50] QGIS Cloud. <https://qgiscloud.com/>.

[51] M. Rahnemoonfar, T. Chowdhury, A. Sarkar, D. Varshney, M. Yari, and R. R. Murphy. Floodnet: A high resolution aerial imagery dataset for post flood scene understanding. *IEEE Access*, 9:89644–89654, 2021. doi: 10.1109/ACCESS.2021.3090981

[52] B. Rieck, U. Fugacci, J. Lukasczyk, and H. Leitte. Clique community persistence: A topological visual analysis approach for complex networks. *IEEE Transactions on Visualization and Computer Graphics*, 24(1):822–831, 2018. doi: 10.1109/TVCG.2017.2744321

[53] A. M. Sainju, W. He, and Z. Jiang. A hidden Markov contour tree model for spatial structured prediction. *IEEE Transactions on Knowledge and Data Engineering*, 34(4):1530–1543, 2022. doi: 10.1109/TKDE.2020.3002887

[54] M. T. Sami, D. Yan, S. Adhikari, L. Yuan, J. Han, Z. Jiang, J. Khalil, and Y. Zhou. Evanet: Elevation-guided flood extent mapping on earth imagery, 2024.

[55] J. Sanyal, S. Zhang, G. Bhattacharya, P. Amburn, and R. Moorhead. A user study to compare four uncertainty visualization methods for 1d and 2d datasets. *IEEE Transactions on Visualization and Computer Graphics*, 15(6):1209–1218, 2009. doi: 10.1109/TVCG.2009.114

[56] M. Sedlmair, M. Meyer, and T. Munzner. Design study methodology: Reflections from the trenches and the stacks. *IEEE Transactions on Visualization and Computer Graphics*, 18(12):2431–2440, 2012. doi: 10.1109/TVCG.2012.213

[57] L. See. A review of citizen science and crowdsourcing in applications of pluvial flooding. *Frontiers in Earth Science*, 7, 2019. doi: 10.3389/feart.2019.00044

[58] C. Songchon, G. Wright, and L. Beevers. The use of crowdsourced social media data to improve flood forecasting. *Journal of Hydrology*, 622:129703, 2023. doi: 10.1016/j.jhydrol.2023.129703

[59] T. Sousbie. The persistent cosmic web and its filamentary structure – I. Theory and implementation. *Monthly Notices of the Royal Astronomical Society*, 414:350 – 383, 06 2011. doi: 10.1111/j.1365-2966.2011.18394.x

[60] V. Sunkara, M. Purri, B. L. Saux, and J. Adams. Street to cloud: Improving flood maps with crowdsourcing and semantic segmentation. *arXiv preprint arXiv:2011.08010*, 2020.

[61] Three.js. <https://github.com/mrdoob/three.js/>.

[62] J. Tierny, G. Favelier, J. A. Levine, C. Gueunet, and M. Michaux. The topology toolkit. *IEEE Transactions on Visualization and Computer Graphics*, 24(1):832–842, 2018. doi: 10.1109/TVCG.2017.2743938

[63] J. Tierny and V. Pascucci. Generalized topological simplification of scalar fields on surfaces. *IEEE Transactions on Visualization and Computer Graphics*, 18(12):2005–2013, 2012. doi: 10.1109/TVCG.2012.228

[64] H. W. W. Sun and X. Zhao. A simplification method for grid-based DEM using topological hierarchies. *Survey Review*, 50(362):454–467, 2018. doi: 10.1080/00396265.2017.1310355

[65] T. A. Wenhao Yu, Yifan Zhang and Z. Chen. An integrated method for DEM simplification with terrain structural features and smooth morphology preserved. *International Journal of Geographical Information Science*, 35(2):273–295, 2021. doi: 10.1080/13658816.2020.1772479

[66] C. Wood, B. Sullivan, M. Iliff, D. Fink, and S. Kelling. ebird: engaging birders in science and conservation. *PLoS Biol*, 9(12):e1001220, Dec. 2011.

[67] Q. Wu, H. Liu, S. Wang, B. Yu, R. Beck, and K. Hinkel. A localized contour tree method for deriving geometric and topological properties of complex surface depressions based on high-resolution topographical data. *International Journal of Geographical Information Science*, 29(12):2041–2060, 2015. doi: 10.1080/13658816.2015.1038719

[68] M. Xie, Z. Jiang, and A. M. Sainju. Geographical hidden Markov tree for flood extent mapping. In *Proceedings of the 24th ACM SIGKDD International Conference on Knowledge Discovery and Data Mining*, KDD '18, p. 2545–2554. Association for Computing Machinery, New York, NY, USA, 2018. doi: 10.1145/3219819.3220053